Symmetry Breaking and Strong Persistent Plasma Currents via Resonant Destabilization of Atoms

C. Brée,[1] M. Hofmann,[2] A. Demircan,[3,4] U. Morgner,[3,4] O. Kosareva,[5] A. Savel'ev,[5] A. Husakou,[6] M. Ivanov,[6] and I. Babushkin[3,6]
[1]Weierstrass Institute, Mohrenstrasse 39, 10117 Berlin, Germany
[2]Virtimo AG, Münzstrasse 5, 10178 Berlin, Germany
[3]Institute for Quantum Optics, Leibniz Universität Hannover, Welfengarten 1, 30167 Hannover, Germany
[4]Hannover Centre for optical Technologies, Nienburger Strasse 17, 30167 Hannover, Germany
[5]Physics Faculty, Lomonosov Moscow State University, Leninskie gory 1-62, 119991 Moscow, Russia
[6]Max Born Institute, Max Born Strasse 2a, 12489 Berlin, Germany
(Received 3 August 2017; revised manuscript received 29 September 2017; published 13 December 2017)

The ionization rate of an atom in a strong optical field can be resonantly enhanced by the presence of long-living atomic levels (so-called Freeman resonances). This process is most prominent in the multiphoton ionization regime, meaning that the ionization event takes many optical cycles. Nevertheless, here, we show that these resonances can lead to rapid subcycle-scale plasma buildup at the resonant values of the intensity in the pump pulse. The fast buildup can break the cycle-to-cycle symmetry of the ionization process, resulting in the generation of persistent macroscopic plasma currents which remain after the end of the pulse. This, in turn, gives rise to a broadband radiation of unusual spectral structure, forming a comb from terahertz to visible. This radiation contains fingerprints of the attosecond electron dynamics in Rydberg states during ionization.

DOI: 10.1103/PhysRevLett.119.243202

The dynamics of atomic photoionization is central to many recent advances in optics and in physics in general, such as attosecond physics and attosecond metrology via high harmonic generation which allowed generation of coherent radiation at frequencies up to many hundreds of eV, dramatically extending the range where coherent ultrashort pulses are available [1,2]. Ionization-induced dynamics can also be used to generate frequencies in the opposite—low-frequency—range, namely in the terahertz (THz) [3–7]. Radiation at THz frequencies can be generated in filaments via wake fields (longitudinal plasma oscillations) [8] or via Cherenkov radiation [9]. However, a much more efficient mechanism is based on the fast steplike tunnel ionization process in strong fields, resulting in formation of persistent macroscopic currents [3–7,10]. For this, one needs to have asymmetric incident waveforms (e.g., using two- or multicolor fields) [4,5,10,11], so that the macroscopic currents created by the positive field half-cycles are not compensated by the currents created during the negative half-cycles. As a result, a persistent current arises and does not disappear after the end of the pulse. The steplike nature of tunnel ionization is of critical importance for this method: in the deep multiphoton regime, as the subcycle steps in, the ionization dynamics gradually disappear, and the method appears to fail [12].

Here, we use the so-called Freeman resonances arising in the multiphoton regime [13], to create a new source of such asymmetry. Freeman resonances appear when the excited atomic states are Stark-shifted by the strong laser field in and out of n-photon resonances. In that case, the population transfer in the atom is dominated by two major competing mechanisms: resonantly enhanced ionization by direct electronic transitions from the ground state into the continuum, and population trapping in high-lying, laser-dressed, and strongly distorted states [14]. The latter can be viewed as the extension of the Kramers-Henneberger concept [15,16] to the Rydberg manifold [17–19].

In this Letter, we show that Freeman resonances produce radiation in a broad frequency range and point out that this radiation contains information about the ionization dynamics. Namely, we show that Freeman resonances are able to produce rather short spikes of ionization even on a subcycle level. This subcycle dynamics breaks the symmetry of the ionization process, leading to the generation of a new comblike structure in a broad frequency range from THz to visible. The comblike structure is a result of interference from different ionization events. The same multi-event structure contains signatures of the electron dynamics "half-way" to the continuum, in particular, of "frustrated tunneling" [19].

First, we will develop an "adiabatic" approach to the problem, which allows us to describe the underlying physics qualitatively. Next, we confirm our model with the direct solution of the time-dependent Schrödinger equation (TDSE).

In the adiabatic regime, we consider the ionization dynamics in a long pulse with a slowly varying envelope. To develop the adiabatic approach, we first find the ionization rate using the non-Hermitian Floquet framework for monochromatic optical fields in the multiphoton regime [20,21]. That is, we assume a strictly periodic field $E = E_0 \cos(\omega_0 t)$ with $\omega_0 = 0.057$ a.u., corresponding to

a wavelength of 800 nm. Then, we search for the Floquet resonances in the eigenvalue problem $(H - i\partial_t)\psi(x,t) = \epsilon_\alpha \psi(x,t)$, where H describes the system Hamiltonian, ϵ_α is the complex quasienergy such that the Floquet eigenfunctions $\Psi = e^{-i\epsilon_\alpha t}\psi$ are quasiperiodic in time: $\Psi(x,t+T) = e^{-i\epsilon_\alpha T}\Psi(x,t)$, $T = 2\pi/\omega_0$. The ionization rate is determined by the inverse lifetime of the resonances $\Gamma_\alpha = -2\mathrm{Im}\epsilon_\alpha$ [22]. We assume that wave function dynamics is governed by a one-dimensional Hamiltonian in velocity gauge

$$H = -\frac{1}{2}\partial_{xx} - \frac{1}{\sqrt{x^2+a^2}} - iA(t)\partial_x. \quad (1)$$

As the considered wavelengths and intensities are well within the validity range of the dipole approximation, this 1D Hamiltonian with a soft-core Coulomb potential [23] is equivalent to the standard one $(p-A)^2 + V$ and reproduces the essential features of radiation and photoelectron spectra in intense laser-matter interaction [24]. Choosing $a = \sqrt{2}$ a. u. allows us to reproduce the ionization energy of atomic hydrogen ($I_p = 13.6$ eV) [21].

Separating the time scales of the slow envelope and the fast carrier oscillation allows us to apply the adiabatic theorem of quantum mechanics [25], which implies that, at each instant of time, the atom remains in the Floquet resonance which is adiabatically connected to the ground state. Also, in this approximation, the population of intermediate levels is negligible and the ionization yield is completely determined by the imaginary part of the Floquet quasienergy. Numerically, the Floquet eigenproblem was solved by discretizing it in a sufficiently large numerical box (we used 200 a.u.), which supports the relevant resonant states.

Dependence of the ionization rate $\Gamma_0[I]$ of the ground-state resonance on the intensity $I = E_0^2/(8\pi\alpha)$ (with the fine-structure constant $\alpha = 1/137$) is shown in Fig. 1(a), exhibiting several narrow resonances. In Fig. 1(b), we show the pulse of the shape $E(t) = E_0 \sin(\omega_0 t)\sin(\pi t/\tau)^2$ with τ being the pulse duration and E_0 the peak field strength [red line in Fig. 1(b) shows the pulse envelope]. The corresponding ionization rate is shown in Fig. 1(b) by a blue curve. One can see that, when the time-varying intensity passes the resonant intensity [e.g., around 15 TW/cm^2, which corresponds to a nine-photon resonance (13.95 eV) between the ground state and the ac-Stark-shifted 7th excited state], sharp spikes in the ionization rate take place, which correspond to the Freeman resonances. The corresponding plasma currents are shown in Figs 1(c) and 1(d) and are obtained from the Drude model without damping via $\partial_t J(t) = \rho(t)E(t)$, with a plasma density ρ governed by a rate equation $\partial_t \rho = \Gamma_0[I(t)](\rho_0 - \rho)$. The current contains fast oscillations reflecting electron dynamics at the frequency ω_0, but the important point is that, after the pulse, the current does not return to zero as would have happened if the resonances were not present.

It is also known that the change of the macroscopic free current J due to ionization can produce radiation (Brunel harmonics) [5,10,12,26–28]. More specifically, if we assume that plasma arises in a small spatial spot, the corresponding field at the observer point will be governed by the expression

$$E_f(t) = g\frac{dJ(t)}{dt} = g\frac{d^2P(t)}{dt^2}, \quad (2)$$

where g is a constant depending on the observation point. We also formally introduced the corresponding polarization as $P(t) = \int^t J(t')dt'$.

As mentioned above, ionization creates harmonics of the pump field only in the case of subcycle ionization dynamics. If the ionization event is much slower than the optical cycle (typically associated with the multiphoton ionization regime), the nonlinearity is "too slow" to create harmonics [12]. From Eq. (2), it follows that, if a persistent current

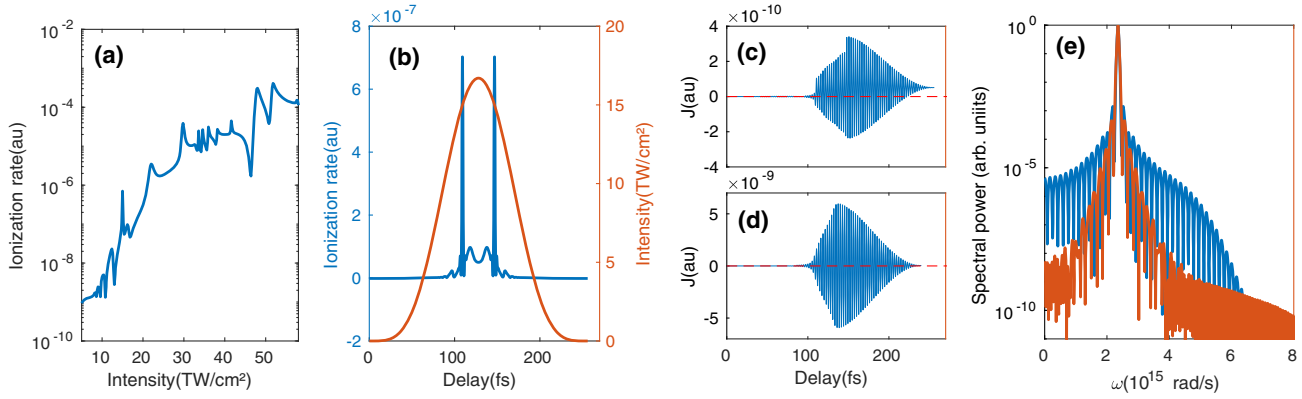

FIG. 1. (a) Ionization rate in dependence of the pump intensity; peaks in ionization rate are Freeman resonances. (b) Intensity (red curve) and the corresponding ionization rate (blue curve) generated by a long pulse of the form described in text, with the wavelength 800 nm, duration 240 fs and peak intensity 17 TW/cm^2. (c), (d) Macroscopic free electron current for 17 TW/cm^2 (c) and 23 TW/cm^2 (d); other parameters as in (b); For the case of 17 TW/cm^2 a persistent current after the field passage is visible. (e) The spectra of the corresponding radiation E_f given by Eq. (2) for the currents shown in (c).

arises (that is, if $J(t=\infty)\neq 0$), there must be a slow component in J which rises on the time scale of the pulse duration. This also leads to the presence of a slow component of $E_f(t)$, i.e., a zeroth harmonic in $E_f(\omega)=\mathcal{F}[E_f(t)]$, where $\mathcal{F}[\cdot]$ is the Fourier transform. To obtain such persistent currents, a certain type of symmetry breaking is necessary; otherwise, the number of electrons going in one direction is exactly the same as the number going in the opposite direction. In the tunnel ionization regime, if the field shape is asymmetric (as, for example, in two-color pulses), the temporal asymmetry of the field waveforms leads to spatial asymmetry of the current and, thus, to generation of macroscopic persistent currents as well as generation of the zeroth harmonic of the pump.

Here, as we observe in Figs. 1(c) and 1(d), the mechanism leading to persistent currents should be closely related to the Freeman resonances. As explained above, this current should also generate low-frequency radiation. By plotting $E_f(\omega)$, defined by Eq. (2), in Fig. 1(e), we see that, indeed, low-frequency components arise. Remarkably, the spectrum contains not only well defined harmonics of the pump, but also a comb of other harmonics in the broad range up to $\omega\sim 5$ fs^{-1}, which corresponds to the visible range. The comb line-to-line distance corresponds to the inverse distance in time between the ionization peaks in Fig. 1(b). The main peak coincides with the central frequency ω_0 of the exciting pulse and corresponds to the motion of free electrons. For comparison, in Fig. 1(d) the current and in Fig. 1(e) the corresponding response spectrum are shown for the intensity of 23 TW/cm^2 (red line). In this case, the Freeman resonances are not excited and the resulting radiation at low frequencies is several orders of magnitude smaller. The structure of the spectrum is the same for other intensities as shown in Fig. 2(c).

The dependence of the corresponding comb on the pulse intensity is presented in Fig. 2. One can clearly see the connection between the excitation of Freeman resonances and the generation of a broadband spectrum. Both the broadband spectrum and the presence of low frequency harmonics indicate that electron ionization dynamics contains a subcycle time scale component, even though we are in the multiphoton ionization regime of the Keldysh parameter $\gamma\gg 1$. The Freeman resonances are so sharp, as a function of the laser intensity, that even the slowly varying field intensity (in our adiabatic picture) passes these resonances very quickly, in less than one optical cycle. This breaks the symmetry and leads to the formation of persistent currents.

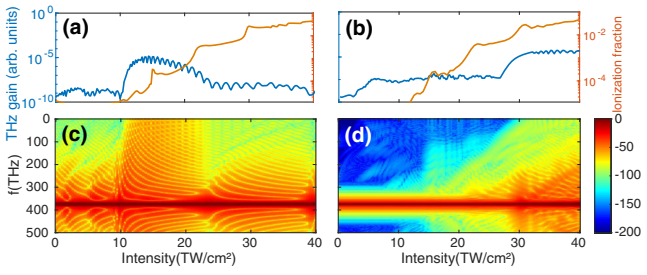

FIG. 2. The generated radiation and its spectrum in dependence on the pulse intensity for the parameters of Fig. 1, assuming the adiabatic procedure as well as the direct solution of the TDSE. (a), (b) Fraction of ionized electrons ρ/ρ_0 (red curves) and the low frequency energy (integrated from 0 to 100 THz) (blue curves) for the case of adiabatic theory (a) and by direct solution of the TDSE (b). (c), (d) Corresponding spectra in dependence of intensity for the adiabatic theory (c) and by direct solution of the TDSE (d).

Formally, as we approach the single-cycle time scale, the adiabatic approximation can no longer be used. Namely, as the ionization rate exhibits very narrow peaks of width ΔI, they are passed in less than an optical cycle if $\Delta I/(dI/dt)<T$. This involves a certain trade-off between adiabatic and nonadiabatic intensity evolution. Therefore, it is necessary to compare our adiabatic model with direct solutions of the full TDSE

$$i\partial_t\psi(x,t)=H\psi(x,t), \tag{3}$$

with the same Hamiltonian Eq. (1). The comparison for the pulse duration 240 fs, as a function of the pulse peak intensity, is shown in Fig. 2. The spectra generated by pulses with different intensities (and the same duration) are shown both for the adiabatic approach [Fig. 2(c)] and for the TDSE simulation [Fig. 2(d)]. The low-frequency part of the radiation integrated over the range between 0 and 100 THz is shown for both cases in Figs. 2(a) and 2(b) (blue lines). Red lines in Figs. 2(a) and 2(b) show the fraction of ionized electrons. One can see that, although the dynamics has some differences, it also has much in common. For example, in the adiabatic case, the Freeman resonance at around 15 TW/cm^2 obviously plays an important role. The influence of this peak is also visible in the case of the TDSE, even though it is much less pronounced. The inverse width of the corresponding resonance is around 800 fs, so that the resonance obviously needs a longer time to fully build up. On the other hand, the peak at around 30 TW/cm^2 plays a significant role in the latter case; this demonstrates that, for the pulse durations we used in Fig. 2, there are still significant differences in the dynamical response of both models.

The situation changes when we consider longer pulses. The result of a more detailed comparison for a longer pulse with the duration of 425.6 fs is shown in Fig. 3. In Fig. 3, we observe cross-correlation frequency-resolved optical gating (XFROG) traces of E_f according to Eq. (2) for the adiabatic and TDSE approaches, respectively. Figure 3(c) shows the ionization rate according to the Floquet theory, while the black solid curves in Figs. 3(d) and 3(e) depict the time dependence of the polarization P. The resonances seen in the adiabatic case are now clearly visible in the TDSE calculation, showing that the agreement between the adiabatic model and the TDSE improves with increasing pulse duration. In Figs. 3(a) and 3(b), the energies of the ionized electrons traveling to the right (blue curves) as well as to the

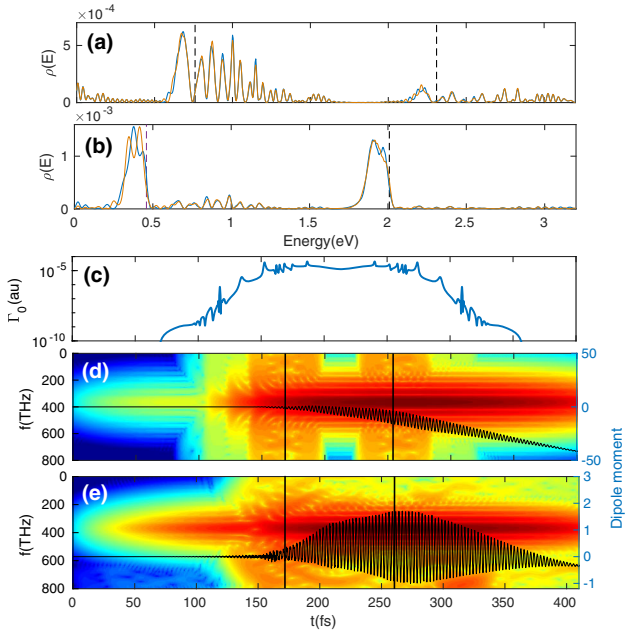

FIG. 3. Comparison of the solution of the TDSE with the adiabatic procedure. (a), (b) Electron energy distributions for electrons traveling to the right (blue curve) and to the left (red curve) calculated with TDSE for a pulse with the intensity 45 TW/cm^2 and pulse duration 425.6 fs (a) and the intensity 50 TW/cm^2 and pulse duration 266.0 fs (b). (c) Ionization rate calculated using Floquet theory vs time. (d), (e) The XFROG diagram of the radiation $E_f(t)$ calculated according Eq. (2) (color scale) and the corresponding polarization $P(t)$ (black line) according to the adiabatic theory (d) and for TDSE calculation (e). Vertical black lines indicate the "center" of the first resonance and the point in time symmetric in respect to the pulse center.

left (red curves) are shown for two different pulse parameters. The peaks deviating from above-threshold ionization peak positions (vertical lines) [13,14,29,30] represent signatures of the Freeman resonances, while the left or right asymmetry gives additional evidence for the existence of the residual currents.

One important point to mention in the solution of the TDSE in Fig. 3 is the remarkable asymmetry with respect to the pulse intensity maximum (see black vertical lines in Fig. 3, indicating temporal points symmetric with respect to the pulse maximum). This is obviously not the case for the adiabatic model. This can be explained by the fact that the first ionization event in the pulse does not only increase the number of the free electrons, but also increases the population of the intermediate states of the system. The second ionization event "probes" this population. In this way, a kind of a pump-probe sequence takes place, where the role of the pump is played by the first ionization event and the role of the probe by the second one. What is probed in this case is the population of highly excited bound states of the atom. To support this conclusion, we plotted, in Fig. 4, the XFROG for an artificial short-range potential, which has the same ionization energy but contains only two bound states. The potential has the form

$$V = -\frac{\exp\left(-x^{10}/\sigma^{10}\right)}{\sqrt{dx^2 + a^2}}, \tag{4}$$

with constants $\sigma = 3$, $d = 0.35$, and $a = 1.549$ (all constants in atomic units). Under these parameters, the second bound state lies around -0.2 a.u. and is also close to the second bound state of the initial potential Eq. (1). One can see from Fig. 4 that the dynamics in the present case is much more symmetric (except for the feature at 450–500 fs, which is caused by plasma losses due to an absorbing boundary in numerical simulations). That is, we can conclude that the asymmetry of the XFROG in Fig. 3 results from the dynamics of the population trapped in high-lying bound states, which are absent in case of our artificial two-level atom.

Finally, to provide additional evidence for the subcycle time scale of the dynamics, we consider the dependence of the effect on the carrier envelope phase (CEP) of the pump pulse. The dynamics of the polarization P is shown in Fig. 5 for two different CEP phases, both for the adiabatic theory [Fig. 5(a)] and for the TDSE [Fig. 5(b)]. By observing the slope of P (since $J = \partial_t P$), one can see that the residual current is strongly CEP dependent, supporting the short-scale dynamics of the process both in the addiabatic and TDSE cases.

The effect observed here lies exactly in the transition regime between the adiabatic and nonadiabatic evolution. If we further increase the pulse duration, the slope of the intensity inside the pulse and, thus, the width of the resonance will increase. As the Freeman resonance width becomes larger than the optical pulse cycle, the transient currents and corresponding radiation disappear as illustrated in Fig. 6. In addition, although the signatures of resonances are still

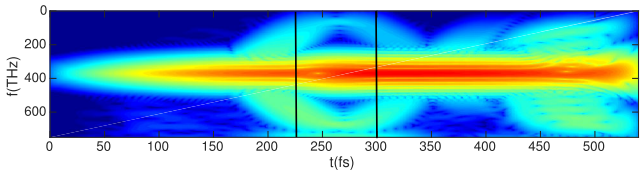

FIG. 4. XFROG diagram of a TDSE simulation for a two-bound-states-atom with the potential given by Eq. (4). Black lines are put at arbitrary points symmetric in respect to the center of the exciting pulse.

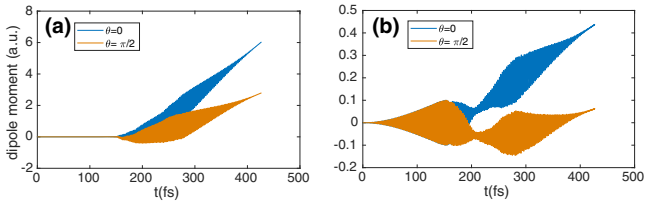

FIG. 5. Dependence of the atomic polarization P on the carrier-envelope phase (CEP) in the adiabatic model (a) and for the direct solution of TDSE (b) for the CEP $\theta = 0$ (blue lines) and $\theta = \pi/2$ (red lines).

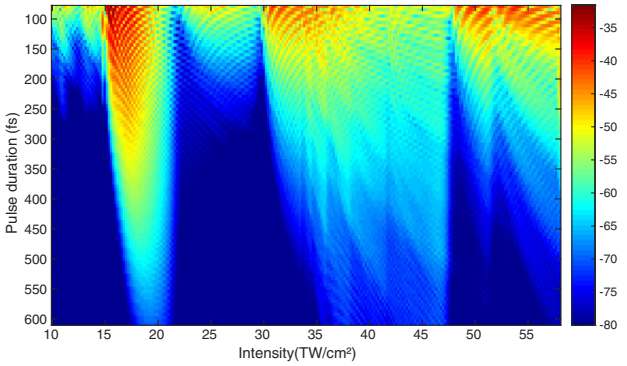

FIG. 6. Dependence of the low frequency radiation component $\sim\omega^2 J(\omega)^2$ on the pulse duration and intensity (note the logarithmic scale) according to the addiabatic model.

visible in Fig. 6 (adiabatic model) for the pulses with the duration $\lesssim$100 fs, they disappear in the TDSE simulations.

In conclusion, we have demonstrated that Freeman resonances lead to spatial symmetry breaking in the generation of free currents of the liberated electrons. This, in turn, leads to the generation of new frequencies in a broad spectral range, similar to Brunel radiation. In particular, it provides a new source of radiation at THz frequencies and a broad comblike spectrum from THz to the visible range. The line-to-line distance of the comb can be controlled by the pulse duration. Even more importantly, this comblike structure, as well as detailed consideration of the corresponding correlation traces, shows that the radiation described here contains the fingerprints of electron transition to the continuum enhanced due to the presence of intermediate resonant states, which can be used to get the information about electron dynamics in conjunction with other established approaches [31–33].

I. B., U. M., and M. I. gratefully acknowledge the support of the Deutsche Forschungsgemeinschaft (DFG) Priority Programme 1840 "Quantum Dynamics in Tailored Intense Fields" (QUTIF) (Grants No. BA 4156/4-1, No. MO 850-19/1, and No. IV 152/7-1). A. S. and O. K. acknowledge support from Russian Science Foundation (Grant No. 16-42-01060). U. M. and A. D. acknowledge support of the DFG (Project No. MO 850-20/1). M. H. and C. B. acknowledge funding by the DFG (Grant No. BR 4654/1). M. I. acknowledges support from the U.S. DOD MURI Grant No. EP/N018680/1.

[1] T. Brabec and F. Krausz, Rev. Mod. Phys. **72**, 545 (2000).
[2] P. B. Corkum, Phys. Rev. Lett. **71**, 1994 (1993).
[3] M. Kreß, T. Löffler, M. D. Thomson, R. Dörner, H. Gimpel, K. Zrost, T. Ergler, R. Moshammer, U. Morgner, J. Ullrich *et al.*, Nat. Phys. **2**, 327 (2006).
[4] K.-Y. Kim, J. H. Glownia, A. J. Taylor, and G. Rodriguez, Opt. Express **15**, 4577 (2007).
[5] K. Y. Kim, A. J. Taylor, J. H. Glownia, and G. Rodriguez, Nat. Photonics **2**, 605 (2008).
[6] M. D. Thomson, M. Kress, T. Löffler, and H. G. Roskos, Laser Photonics Rev. **1**, 349 (2007).
[7] K. Reimann, Rep. Prog. Phys. **70**, 1597 (2007).
[8] P. Sprangle, J. R. Peñano, B. Hafizi, and C. A. Kapetanakos, Phys. Rev. E **69**, 066415 (2004).
[9] C. D'Amico, A. Houard, M. Franco, B. Prade, A. Mysyrowicz, A. Couairon, and V. T. Tikhonchuk, Phys. Rev. Lett. **98**, 235002 (2007).
[10] I. Babushkin, S. Skupin, A. Husakou, C. Khler, E. Cabrera-Granado, L. Berg, and J. Herrmann, New J. Phys. **13**, 123029 (2011).
[11] P. G. Martínez, I. Babushkin, L. Bergé, S. Skupin, E. Cabrera-Granado, C. Köhler, U. Morgner, A. Husakou, and J. Herrmann, Phys. Rev. Lett. **114**, 183901 (2015).
[12] I. Babushkin, C. Brée, C. M. Dietrich, A. Demircan, U. Morgner, and A. Husakou, J. Mod. Opt. **64**, 1078 (2017).
[13] R. R. Freeman, P. H. Bucksbaum, H. Milchberg, S. Darack, D. Schumacher, and M. E. Geusic, Phys. Rev. Lett. **59**, 1092 (1987).
[14] G. N. Gibson, R. R. Freeman, and T. J. McIlrath, Phys. Rev. Lett. **69**, 1904 (1992).
[15] M. Pont and M. Gavrila, Phys. Rev. Lett. **65**, 2362 (1990).
[16] J. Eberly and K. Kulander, Science **262**, 1229 (1993).
[17] M. Richter, S. Patchkovskii, F. Morales, O. Smirnova, and M. Ivanov, New J. Phys. **15**, 083012 (2013).
[18] H. Zimmermann, S. Patchkovskii, M. Ivanov, and U. Eichmann, Phys. Rev. Lett. **118**, 013003 (2017).
[19] T. Nubbemeyer, K. Gorling, A. Saenz, U. Eichmann, and W. Sandner, Phys. Rev. Lett. **101**, 233001 (2008).
[20] S.-I. Chu, in *Advances in Chemical Physics* (John Wiley & Sons, Inc., New York, 2007), pp. 739–799.
[21] M. Hofmann and C. Brée, J. Phys. B **49**, 205004 (2016).
[22] R. M. Potvliege and R. Shakeshaft, Phys. Rev. A **40**, 3061 (1989).
[23] R. L. Hall, N. Saad, K. D. Sen, and H. Ciftci, Phys. Rev. A **80**, 032507 (2009).
[24] E. Cormier and P. Lambropoulos, J. Phys. B **29**, 1667 (1996).
[25] M. Born and V. Fock, Z. Phys. **51**, 165 (1928).
[26] F. Brunel, J. Opt. Soc. Am. B **7**, 521 (1990).
[27] T. Balčiūnas, D. Lorenc, M. Ivanov, O. Smirnova, A. Zheltikov, D. Dietze, K. Unterrainer, T. Rathje, G. Paulus, A. Baltuška, and S. Haessler, Opt. Express **23**, 15278 (2015).
[28] T. Balčiūnas, A. Verhoef, A. Mitrofanov, G. Fan, E. Serebryannikov, M. Ivanov, A. Zheltikov, and A. Baltuška, Chem. Phys. **414**, 92 (2013).
[29] R. Wiehle, B. Witzel, H. Helm, and E. Cormier, Phys. Rev. A **67**, 063405 (2003).
[30] G. D. Gillen and L. D. Van Woerkom, Phys. Rev. A **68**, 033401 (2003).
[31] M. Drescher, M. Hentschel, R. Kienberger, M. Uiberacker, V. Yakovlev, A. Scrinzi, T. Westerwalbesloh, U. Kleineberg, U. Heinzmann, and F. Krausz, Nature (London) **419**, 803 (2002).
[32] M. Uiberacker, T. Uphues, M. Schultze, A. J. Verhoef, V. Yakovlev, M. F. Kling, J. Rauschenberger, N. M. Kabachnik, H. Schroder, M. Lezius, K. L. Kompa, H. G. Muller, M. J. J. Vrakking, S. Hendel, U. Kleineberg, U. Heinzmann, M. Drescher, and F. Krausz, Nature (London) **446**, 627 (2007).
[33] A. M. Zheltikov, A. A. Voronin, M. Kitzler, A. Baltuška, and M. Ivanov, Phys. Rev. Lett. **103**, 033901 (2009).